biotic resistance and virulence factors. The finding of a connection between bacterial conjugation and biofilm formation suggests that an important ecological consequence of the use of antibiotics and biocides in clinical medicine and agriculture may have been the selection of plasmid-bearing strains that are more likely to form a biofilm. Because biofilms are a common cause of persistent nosocomial infections that are difficult to eradicate owing to innate physiological properties[14], this aspect may prove to be of relevant medical significance in addition to the conjugational spread of virulence factors themselves. □

Methods

Bacterial strains and plasmids

Bacterial strains are listed in Table 1 and were provided by the Collection of the Institut Pasteur (http://www.pasteur.fr/applications/CIP/) and the Unité des Agents Antibactériens (P. Courvalin and G. Gerbaud).

Biofilm

All experiments were performed in triplicate in 0.4% glucose M63B1 minimal medium at 37 °C. Continuous 60-ml microfermenters with four liquid and gas sampling ports (Pasteur Institute's Laboratory of Fermentation) were configured as continuous-flow culture bioreactors with a 40 ml h^{-1} flow rate (F). 10^8 bacterial inocula from overnight precultures grown in glucose minimal medium with required antibiotics were used to inoculate microfermenters, which were then cultivated for 3–48 h. The culture volume (V) was constant and the imposed dilution rate (D) was $D = F/V = 0.66\ h^{-1}$. Hence, the theoretical generation time (T) required for constant density culture in the microfermenter was $T = \ln 2/D = 1.05$ h. The average generation time calculated in exponential batch culture for *E. coli* strains MG1655 and BM21 was 1.3 h. Therefore, the high input rate of fresh, diluting medium used in our experimental model was imposed to avoid any significant planktonic growth. Stirring was assured by aeration with sterile pressed air (0.3 bar). Submerged, removable Pyrex slides (total area of 22.4 cm^2) served as growth substratum.

Microscopy and image analysis

Biofilm development was recorded with a Nikon Coolpix 950 digital camera. Epifluorescence, phase contrast and transmitted light microscopy were acquired with a Leitz Dialux 20EB microscope equipped with ×25 to ×100 objectives. Scanning confocal microscopy was performed at the confocal microscopy station of the Pasteur Institute.

Non-polar deletion of the *traA* gene

A non-polar mutation deleting the entire *traA* gene was created by allelic exchange[15] using the primers TraAGB-5: 5′-AGGGAGGCAGATAAAGAGGAAGATATAACATTTAATACA CTCTAGTTTTATTCATTTATCCGAAATTGAGGTAACTTATGAAAGCCACGTTGTG TCTCAA-3′ and TraAGBnp-3: 5′-GCGGCTCTGGTTGGTCAGTGTTTCCGGGAAACG ATATTTCTTAAGTTTATTCTCGTCTCCCGACATCGTTTTATTTCCTGTTAGAAAAA CTCATCGAGCA-3′, and *aphA* gene (kanamycin resistance) from Tn*903* as template. The mutation was verified by PCR analysis.

Cloning of the *traA* gene

pTraA was constructed by PCR amplification of *traA* from strain TG1 using the primers TraAecorbs-5: 5′-AAAGAATTCGAAATTGAGGTAACTTATGAATGC-3′ and TraAH3-3: 5′-CCCAAGCTTCGTTTTATTTCCTGTCAGAG-3′. I verified the nucleotide sequence of the construction.

Biofilm co-inoculation procedures

A preculture of a recipient strain BM21 (nal^r (nalidixic acid resistant)) was inoculated for 24 h and then co-inoculated with MG1655-S R1 (St^r (streptomycin resistant), Ap^r (ampicillin resistant) and Km^r (kanamycin resistant)) for another 24 h. Pyrex slides were removed and cenrifuged in 15 ml of fresh M63B1 medium for 1 min. The number of colony-forming units was determined by plating serial dilutions of the resuspensions on medium supplemented with nalidixic acid (for recipient BM21 scoring), streptomycin, ampicillin, kanamycin (for donor MG1655-S R1 scoring), nalidixic acid, ampicillin and kanamycin (for BM21 R1 transconjugant scoring), and without antibiotic (for total cell scoring). Co-inoculation with BM21 strains carrying the plasmids described in Table 1 were generated using MG1655-S as recipient bacteria.

Received 8 March; accepted 6 June 2001.

1. de la Cruz, I. & Davies, I. Horizontal gene transfer and the origin of species: lessons from bacteria. *Trends Microbiol.* **8,** 128–133 (2000).
2. Lederberg, J. & Tatum, E. L. Gene recombination in *Escherichia coli*. *Nature* **158,** 558 (1946)..
3. Ochman, H., Lawrence, J. G. & Groisman, E. A. Lateral gene transfer and the nature of bacterial innovation. *Nature* **405,** 299–304 (2000).
4. Costerton, J. W., Lewandowski, Z., Caldwell, D. E., Korber, D. R. & Lappin-Scott, H. M. Microbial biofilms. *Annu. Rev. Microbiol.* **49,** 711–745 (1995).
5. Hausner, M. & Wuertz, S. High rates of conjugation in bacterial biofilms as determined by quantitative in situ analysis. *Appl. Environ. Microbiol.* **65,** 3710–3713 (1999).
6. Christensen, B. B. *et al.* Establishment of new genetic traits in a microbial biofilm community. *Appl. Environ. Microbiol.* **64,** 2247–2255 (1998).
7. O'Toole, G. A. & Kolter, R. Flagellar and twitching motility are necessary for *Pseudomonas aeruginosa* biofilm development. *Mol. Microbiol.* **30,** 295–304 (1998).
8. Pratt, L. A. & Kolter, R. Genetic analyses of bacterial biofilm formation. *Curr. Opin. Microbiol.* **2,** 598–603 (1999).
9. Frost, L. S., Ippen-Ihler, K. & Skurray, R. A. Analysis of the sequence and gene products of the transfer region of the F sex factor. *Microbiol. Rev.* **58,** 162–210 (1994).
10. Ried, G. & Henning, U. A unique amino acid substitution in the outer membrane protein OmpA causes conjugation deficiency in *Escherichia coli* K-12. *FEBS Lett.* **223,** 387–390 (1987).
11. Lundquist, P. D. & Levin, B. R. Transitory derepression and the maintenance of conjugative plasmids. *Genetics* **113,** 483–497 (1986).
12. Watnick, P. & Kolter, R. Biofilm, city of microbes. *J. Bacteriol.* **182,** 2675–2679 (2000).
13. Bergstrom, C. T., Lipsitch, M. & Levin, B. R. Natural selection, infectious transfer and the existence conditions for bacterial plasmids. *Genetics* **155,** 1505–1519 (2000).
14. Costerton, J. W., Stewart, P. S. & Greenberg, E. P. Bacterial biofilms: a common cause of persistent infections. *Science* **284,** 1318–1322 (1999).
15. Chaveroche, M. K., Ghigo, J. M. & d'Enfert, C. A rapid method for efficient gene replacement in the filamentous fungus aspergillus nidulans. *Nucleic Acids Res.* **28,** E97 (2000).
16. Couturier, M., Bex, F., Bergquist, P. L. & Maas, W. K. Identification and classification of bacterial plasmids. *Microbiol. Rev.* **52,** 375–395 (1988).
17. Bukhari, A. I., Shapiro, J. A. & Adhya, S. L. (eds) *DNA Insertion Elements, Plasmids and Episomes* 601–656 (Cold Spring Harbor Laboratory, Cold Spring Harbor, 1977).
18. Bradley, D. E., Taylor, D. E. & Cohen, D. R. Specification of surface mating systems among conjugative drug resistance plasmids in *Escherichia coli* K-12. *J. Bacteriol.* **143,** 1466–1460 (1980).
19. Frost, L. S. in *Bacterial conjugation* (ed. Clewel, D. B.) 189–221 (Plenum, New York, 1993).

Supplementary Information is available on *Nature's* World-Wide Web site (http://www.nature.com) or as paper copy from the London editorial office of *Nature*.

Acknowledgements

I am grateful to C. Wandersman for support and constant interest during the course of this work. I also thank D. Mazel, G. Gerbaud and P. Courvalin for providing the plasmids and strains used in this study; A. Idja and P. Roux for technical assistance; R. Longin for providing facilities of the Pasteur Institute Laboratory of Fermentations; and D. Mazel, E. Stewart, D. A. Rowe-Magnus and P. Delepelaire for helpful discussions and critical reading of the manuscript. This work was supported by grants from the Programme de Recherche Fondamentale en Microbiologie et Maladie Infectieuses, réseau Infections Nosocomiales (MENRT) and the Pasteur Institute.

Correspondence and requests for material should be addressed to the author (e-mail: jmghigo@pasteur.fr).

Force can overcome object geometry in the perception of shape through active touch

Gabriel Robles-De-La-Torre & Vincent Hayward

McGill University, Center for Intelligent Machines, Montréal, Canada H3A 2A7

Haptic (touch) perception normally entails an active exploration of object surfaces over time. This is called active touch[1–3]. When exploring the shape of an object, we experience both geometrical[4] and force cues. For example, when sliding a finger across a surface with a rigid bump on it, the finger moves over the bump while being opposed by a force whose direction and magnitude are related to the slope of the bump[5]. The steeper the bump, the stronger the resistance. Geometrical and force cues are correlated, but it has been commonly assumed that shape perception relies on object geometry alone. Here we show that regardless of surface geometry, subjects identified and located shape features on the basis of force cues or their correlates. Using paradoxical stimuli, for example combining the force cues of a bump with the geometry of a hole, we found that subjects perceived a bump. Conversely, when combining the force cues of a hole with the geometry of a bump, subjects typically perceived a hole.

In two experiments, human subjects explored surfaces by touch

using an apparatus that allowed us to separate force cues from surface geometry. Subjects explored the shape of surfaces through a manipulandum placed behind a curtain (Fig. 1). Subjects pressed down on the plate of the manipulandum with their index fingers while smoothly rolling it on the surfaces. There were three interchangeable physical surfaces. One surface was flat, one had a bump, and another had a hole; the latter two had a gaussian profile that was 0.3 cm high/deep and 4 cm wide. The plate was constrained to remain horizontal, and its vertical position was entirely determined by the geometry of the physical surfaces. A force-feedback haptic interface could produce a horizontal force as a function of the measured vertical component F_{sy} (the force applied vertically by the subjects, Fig. 2a) and of the plate's horizontal position (Fig. 1, Methods). The force of the interface interacted with the force returned by the physical surface. The interface's force was called a 'virtual surface' because it provided the same horizontal force component that an equivalent physical surface would return, regardless of the manipulandum's vertical position. For example, when subjects explored a physical bump or hole (Fig. 2a and b), they experienced a horizontal force F_{px}. When subjects explored a flat surface combined with a virtual bump or hole, they experienced the same horizontal force F_{px} (Fig. 2c, grey, dashed curve), but the manipulandum moved in a straight line (Fig. 2c, black line). In another example, the horizontal force component from a physical bump was cancelled out ('force-masked', Methods) by a spatially aligned virtual hole (Fig. 2d). Here, the vertical position of the manipulandum followed the geometry of the bump (Fig. 2d, black curve), but subjects did not experience horizontal force components (Fig. 2d, grey, dashed line). The manipulandum would stay in equilibrium on a slope regardless of how much the subjects pushed on it, just as if they were exploring a flat surface.

In experiment 1, we used the paradoxical stimuli just described to investigate whether subjects classified and located shape features by following geometrical or horizontal force cues. Subjects were tested using seven different conditions. In condition 1, only flat surfaces were presented. In condition 2, the flat surfaces were combined with virtual bumps, and in condition 3 with virtual holes (Fig. 2c). In condition 4 there were only ordinary physical bumps, and in condition 5 ordinary physical holes (Fig. 2b). In condition 6, the physical bumps were force-masked by virtual holes, and control virtual bumps were randomly placed elsewhere (Fig. 2e). Condition 7 mirrored condition 6 (Fig. 2e). The positions of physical and virtual surfaces were uncorrelated in conditions 6 and 7. The probability of classifying a stimulus as a hole or a bump was calculated for each subject under all conditions. The stimulus localization performance of the subjects was measured by the correlation between stimulus location and subjects' positioning of the manipulandum (Methods).

The flat surfaces were classified as flat (Fig. 3a, b, condition 1). Virtual bumps, combined with the flat surface, were classified as bumps ($P < 0.001$; Fig. 3a, condition 2), and were accurately located (Fig. 3c). Virtual holes, combined with the flat surface, were also identified as holes ($P < 0.001$; Fig. 3b, condition 3) and were precisely located (Fig. 3d). When physical holes or bumps were presented alone, subjects also easily identified and located them (Fig. 3a–d, conditions 4 and 5). There was no significant difference in subjects' identification and localization performance when exploring physical or virtual surfaces. However, when force-masked physical holes or bumps were combined with virtual surfaces, subjects' features localization was affected drastically. Subjects' identification performance remained the same (Fig. 3a, b, conditions 6 and 7), but most subjects tracked the control virtual

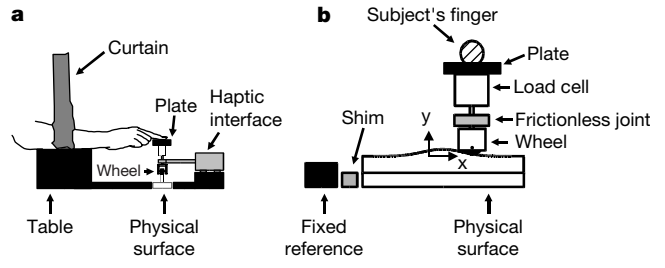

Figure 1 Side (**a**) and front (**b**) views of the apparatus. Subjects pressed down on the manipulandum's plate and rolled it sideways (*x*-axis in **b**) to explore the shape of an interchangeable physical surface. The entire workspace was hidden from view behind a black curtain. The manipulandum was connected to a haptic interface (Methods) that operated silently.

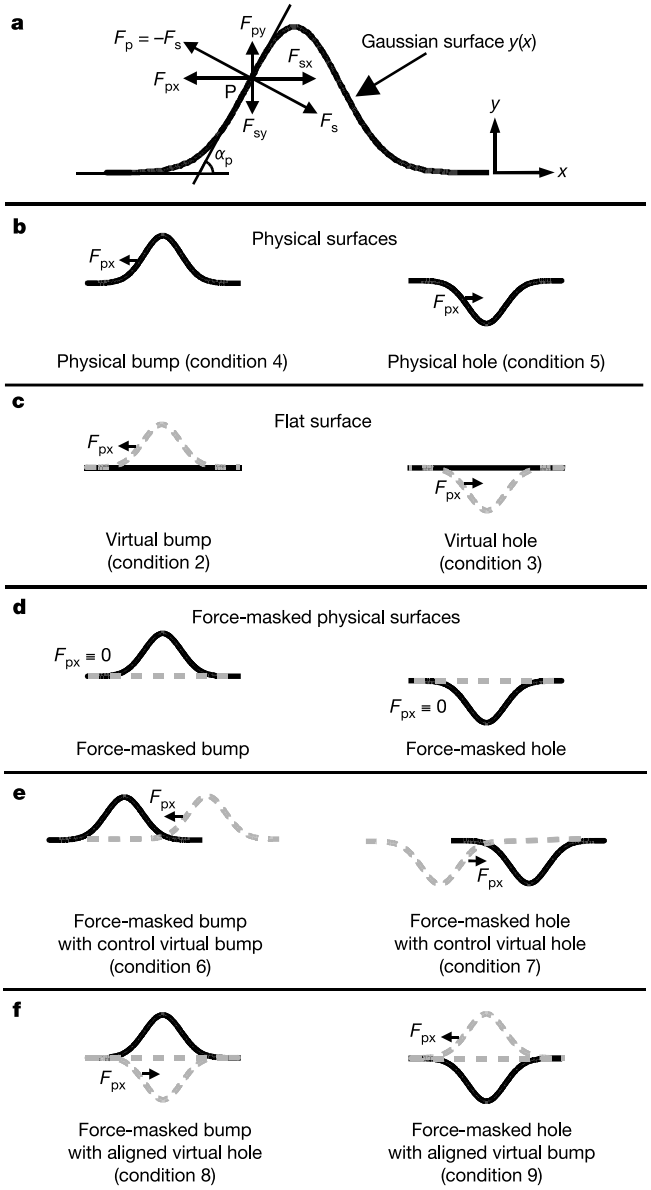

Figure 2 Experimental conditions 2–9. When the haptic interface was turned off, subjects experienced F_{px}, the horizontal force component that depends on surface geometry (**a**, **b**). Equivalent forces (**c**–**f**) were produced by the interface to generate stimuli with uncorrelated force (grey, dashed curves) and geometric cues (black curves). The force cues from virtual bump/hole stimuli (**c**) were equivalent to those of physical bumps/holes, but provided the geometrical cues of a flat surface. Force-masked stimuli (**d**–**f**) were used to create physical bumps/holes with spatially uncorrelated cues (**e**), physical holes with a bump's force cues, and physical bumps with a hole's force cues (**f**).

surfaces instead of the force-masked physical holes or bumps (Fig. 3c, d, conditions 6 and 7, thick circles, $P < 0.009$ for virtual bumps and $P < 0.001$ for virtual holes; see also Supplementary Information). The physical bumps or holes provided geometric but not horizontal force information to subjects, whereas the virtual surfaces provided force but not geometrical information. Given the subjects' instructions (see Methods), this suggests that the control virtual holes or bumps seemed deeper or bigger than the force-masked physical holes or bumps. Horizontal force was used instead of geometry to identify and locate shape features. This happened when geometrical information was absent (conditions 2 and 3) and when object geometry did not correlate with force (conditions 6 and 7). One subject displayed a significant localization performance when tracking force-masked bumps (Fig. 3c, condition 6). The position of the force-masked and virtual bumps presented to this subject had a spurious, non-significant correlation of 0.32 that explained the subject's significant tracking. Only this subject was exposed to spurious correlations. However, the subject clearly followed the virtual bumps and not the force-masked physical bumps (Supplementary Information). Some subjects located the force-masked shapes in some trials, and the control virtual shapes in other trials. These were subjects with significant localization correlations equal to or below 0.65 when tracking virtual bumps (Fig. 3c, condition 6; Supplementary Information), or virtual and force-masked holes (Fig. 3d, condition 7; Supplementary Information).

If subjects relied on force information to identify and locate shape features, then an easily identified and located physical bump should be perceptually transformed into a hole by combining it with the force cues of a hole. An equivalent perceptual reversal should happen for a physical hole. Experiment 2 explored this idea with a new group of subjects. Again, they were tested using condition 1 (flat surfaces, no virtual surface), conditions 2 and 3 (virtual surfaces, Fig. 2c), and conditions 4 and 5 (physical surface alone,

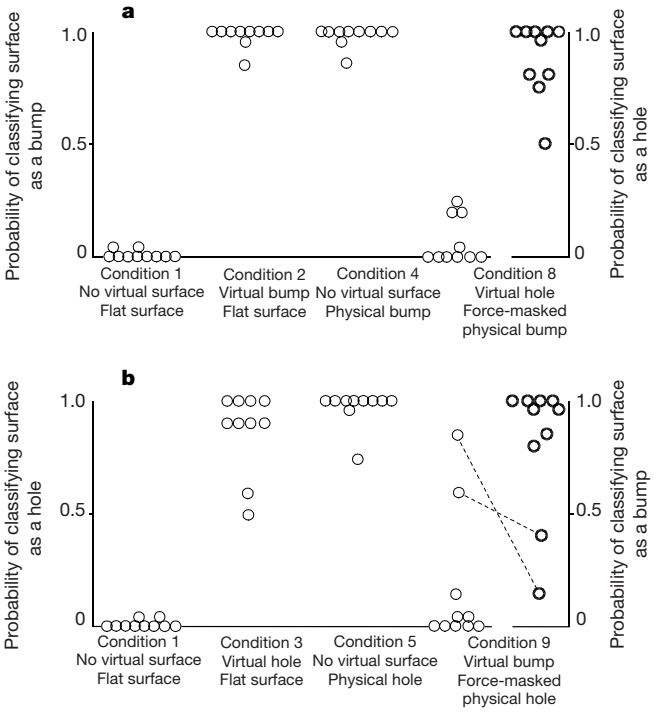

Figure 4 Force perceptually transformed geometrical shape. Each symbol represents data from a single subject. Subjects easily classified physical and virtual surfaces (**a**, **b**, conditions 1–5) as bumps or holes. However, when force-masked physical bumps coincided with virtual holes, stimuli were classified as holes (**a**, condition 8, thick circles, right axis). A mirrored perceptual change occurred when force-masked physical holes coincided with virtual bumps (**b**, condition 9, thick circles, right axis). Two subjects identified the physical holes but took the longest average times to make a judgement (text). Dotted lines join data points corresponding to the same subjects.

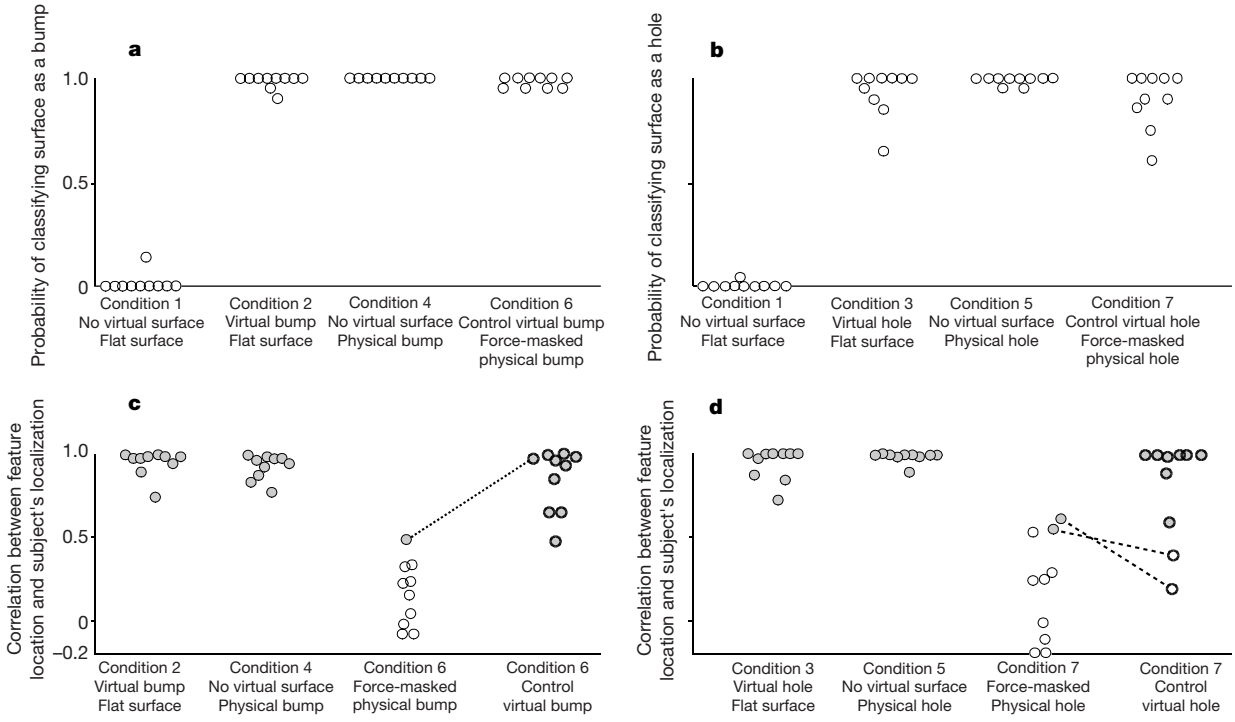

Figure 3 Subjects used force to identify or locate shape features. Each symbol represents data from one subject. Subjects easily classified stimuli as bumps or holes when a virtual surface or flat physical surface combination was presented, or when virtual and physical surfaces coexisted, but not when a flat surface was presented alone (**a**, **b**). Subjects tracked the position of physical and virtual surfaces (**c**, **d**, conditions 2–5). However, when virtual surfaces and force-masked physical surfaces were presented side by side, most subjects tracked the control virtual surfaces (**c**, **d**, conditions 6 and 7, thick circles). Dotted lines link the data from the same subject. Grey circles indicate significant correlations ($P < 0.05$) between stimulus position and subjects' localization.

Fig. 2b). Conditions 6 and 7 were replaced by conditions 8 and 9. In condition 8, two virtual holes coincided with a physical bump (Fig. 2f). One virtual hole force-masked the physical bump, and the other provided a hole's horizontal force cues. As a result, the net horizontal force helped subjects to ascend slopes. Condition 9 mirrored condition 8 (Fig. 2f).

Subjects easily identified or located physical bumps when there was no virtual surface (Fig. 4a, condition 4). However, when physical bumps were presented together with the force cues of a hole, subjects reversed their identification performance. These stimuli were not classified as bumps (Fig. 4a, condition 8, thin circles, left axis) but as holes ($P < 0.001$, Fig. 4a, condition 8, thick circles, right axis). One subject identified these stimuli as either flat surfaces or holes with a 50% probability. Physical holes were easily identified or located when presented alone (Fig. 4b, condition 5). But combinations of physical holes and virtual bumps were classified as bumps ($P < 0.009$, Fig. 4b, condition 9, thick circles, right axis), not as holes (Fig. 4b, condition 9, thin circles, left axis). Two subjects behaved differently (Fig. 4b, data points joined by dotted lines). These two subjects took the longest average time to explore these stimuli: 20.4 s and 21 s, compared to 6.8–16.7 s (mean 11.4 s) for all other subjects. This suggested that these stimuli were ambiguous to subjects and that, over longer exploration times, geometrical cues may contribute more to subjects' perception. As in experiment 1, there was no significant difference in subjects' ability to locate any of the stimuli categories (data not shown).

Our results indicate that force or force-related information (for example, hand/finger velocity) can overcome geometrical information, such as slope, to determine shape perception through active touch. This happened for maximum slope differences well above reported thresholds: 5.71 degrees compared to 0.57 (ref. 6) and 3–4 degrees (ref. 4). Our subjects used a combination of finger, wrist and forearm movements to explore stimuli. Kinesthesia research[7–9] suggests that subjects may have easily detected these movements, particularly those of the metacarpophalangeal joint of the index finger[9]. Our results indicate that most subjects did not use this information to classify/locate shape features. This suggests that the nervous system may sense both force and kinesthetic cues for shape perception, but processes these cues separately and/or weighs them differently.

Because classification or localization performance for physical and virtual surfaces was equivalent, virtual surfaces can be considered as illusory haptic shapes. Informal observations suggest that similar phenomena occur when the manipulandum is used with the wrist, the elbow and the big toe. The reader may reproduce the approximate conditions of our experiments with simple materials (see http://www.cim.mcgill.ca/~roblesg/vsdemo.html). □

Methods

Physical shapes

When subjects explored a frictionless physical surface $y(x)$, they applied a force F_s (Fig. 2a). The surface returned a normal force $F_p = -F_s$ at **P**. F_{px} and F_{py} (the horizontal and vertical components of F_p) are related: $F_{px} = F_{py} \tan[\alpha_p(x)]$. For a profile $y(x)$, $\tan[\alpha_p(x)] = dy/dx$. The profile used was gaussian, $y(x) = k \exp[-(x - x_{ploc})^2/w^2]$, where x_{ploc} is the position of the profile in the workspace, $w = 2$ cm, $k = 0.3$ cm for a bump and $k = -0.3$ cm for a hole. Interchangeable shims could precisely locate the profile at $x_{ploc} = 0$, 1.56 or 2.2 cm. The physical surfaces were precision-machined out of hard plastic.

Virtual shapes and force masking

A force-feedback haptic interface produced the computer-controlled horizontal force F_v that interacted with F_s and F_p through a frictionless point (Fig. 1). Under low-velocity conditions, F_v, F_s and F_p balanced: $F_s + F_p + F_v = 0$. Along the x and y directions, $F_{sx} + F_{px} + F_v = 0$ and $F_{sy} + F_{py} = 0$. A load cell (Fig. 1) measured $F_{py} = -F_{sy}$ (Fig. 2a) and the haptic interface measured x, the horizontal position of the plate. The device was programmed to produce $F_v = F_{sy} \tan[\alpha_p(x - x_{ploc})] + F_{py} \tan[\alpha_v(x - x_{vloc})]$. Because the force experienced by a subject in the horizontal direction was $F_{sx} = -F_{px} - F_v$, the first term of F_v defined a virtual surface that cancelled out ('force-masked') the horizontal component of the force returned by a physical surface located at x_{ploc}. The second term of F_v defined a virtual surface located at x_{vloc}. The physical/virtual surface shapes were aligned when $x_{ploc} = x_{vloc}$. In conditions 2 and 3 (both experiments), the first term of F_v was not used.

Force-feedback haptic interface

A PenCAT/Pro (Immersion Canada Inc.) interface produced F_v and measured x. The interface had negligible friction and operated silently. Manipulandum's position/forces were sampled at 1 kHz. The force feedback was updated at the same rate. A manipulandum similar to ours was theoretically described by Minsky[10] to illustrate a physical model of simulated textures.

Experimental procedure

Subjects gave informed consent, were paid to participate and naive to the purpose of the experiment, did not have calluses on their right index finger nor report any hand injury/disease. Ten right-handed subjects participated in experiment 1; four males and six females, ages 19–31. Ten new right-handed subjects participated in experiment 2; six males and four females, ages 18–31. Handedness was evaluated by using a standard questionnaire[11]. In each trial, a stimulus was randomly selected from an experimental condition. The manipulandum's position was randomly set either to the right or left end of the workspace. A subject's index finger was placed on the centre of the manipulandum's plate (Fig. 1). Subjects were instructed to locate the highest/lowest point of the highest/deepest perceived bump/hole. There was no time limit for exploration, but proceeding quickly was encouraged. After locating the feature, subjects did not change the manipulandum's position. Subjects ended the trial by pressing a button on a computer keyboard to identify the located feature. Buttons were labelled 'bump', 'hole' and 'flat'. No feedback was given. Subjects withdrew their fingers from the manipulandum after pressing the button. Only physical surfaces were presented during 25 practice trials. During practice, the shims were not used and the surface's position was randomly varied across the workspace. Each subject proceeded to complete 140 experimental trials. Each experimental condition was tested 20 times. Subjects had periodic breaks after every 50 trials, but could rest at any time. A typical experiment lasted about one hour and fifty minutes.

Data analysis

For each experimental condition, subjects' localization performance was measured by the Pearson correlation coefficient between physical/virtual surface location and subjects' final manipulandum position. If a stimulus provided the force cues of a bump (virtual or physical) but was classified as a hole or as a flat surface, the trial was not used to compute the correlation. Conversely, a trial was not used for correlation calculations if the stimulus provided the force cues of a hole (virtual or physical), but was classified as a bump or as a flat surface. Subjects' classification performance was measured by calculating the probabilities of classifying a stimulus as a bump or as a hole, respectively. Multivariate ANOVA tests and planned comparisons evaluated within-subject effects of each condition.

Received 28 November 2000; accepted 17 May 2001.

1. Gibson, J. J. Observations on active touch. *Psychol. Rev.* **69,** 477–491 (1962).
2. Loomis, J. M. & Lederman, S. J. in *Handbook of Perception and Human Performance* Vol. 2 *Cognitive Processes and Performance* (ed. Boff, K. R. *et al.*) Ch. 31, 1–41 (New York, Wiley, 1986).
3. Lederman, S. J. & Klatzky, R. L. Hand movements: a window into haptic object recognition. *Cogn. Psychol.* **19,** 342–368 (1987).
4. Pont, S. C., Kappers, A. M. L. & Koenderink, J. J. Similar mechanisms underlie curvature comparison by static and dynamic touch. *Percept. Psychophys.* **61,** 874–894 (1999).
5. Robles-De-La-Torre, G. & Hayward, V. in *Proc. ASME Dynamics Systems and Control Division* Vol. 2 (ed. Nair, S. S.) 1081–1085 (The American Society of Mechanical Engineers, New York, 2000).
6. Gordon, I. E. & Morison, V. The haptic perception of curvature. *Percept. Psychophys.* **31,** 446–450 (1982).
7. Taylor, J. L. & McCloskey, D. I. Detection of slow movements imposed at the elbow during active flexion in man. *J. Physiol.* **457,** 503–513 (1992).
8. Hall, L. A. & McCloskey, D. I. Detections of movements imposed on finger, elbow and shoulder joints. *J. Physiol.* **335,** 519–533 (1983).
9. Clark, F. J., Burgess, R. C. & Chapin, J. W. Proprioception with the proximal interphalangeal joint of the index finger. Evidence for a movement sense without a static-position sense. *Brain* **109,** 1195–1208 (1986).
10. Minsky, M. *Computational Haptics: The Sandpaper System for Synthesizing Texture for a Force-Feedback Display.* PhD dissertation. Massachusetts Institute of Technology (1995).
11. Coren, S. *The Left-hander Syndrome* (Maxwell Macmillan International, New York, 1992).

Supplementary information is available on *Nature*'s World-Wide Web site (http://www.nature.com) or as paper copy from the London editorial office of *Nature*.

Acknowledgements

We thank M. Cynader, B. Frost and L. Requadt for helpful comments, and D. Pavlasek and J. Boka for help in designing/building the manipulandum and surfaces. The research was funded by Canada's Network of Centers of Excellence programme, Institute for Robotics and Intelligent Systems, and the Natural Sciences and Engineering Research Council of Canada.

Correspondence and requests for materials should be addressed to G.R. (e-mail: roblesg@cim.mcgill.ca).